Available online at www.sciencedirect.com

ScienceDirect

Ceramics International 40 (2014) 5085–5090

CERAMICS INTERNATIONAL

www.elsevier.com/locate/ceramint

Short communication

Shape-controlled synthesis of $MnWO_4$ nanocrystals by a surfactant-free hydrothermal method

Yonggang Wang[a,*], Linlin Yang[a], Yujiang Wang[a], Xiaofeng Wang[a], Gaorong Han[b]

[a]Department of Materials Science and Engineering, Luoyang Institute of Science and Technology, Luoyang 471023, PR China
[b]State Key Laboratory of Silicon Materials, Department of Materials Science and Engineering, Zhejiang University, Hangzhou 310027, PR China

Received 21 August 2013; received in revised form 25 September 2013; accepted 26 September 2013
Available online 3 October 2013

Abstract

In this paper, we report the obtention of $MnWO_4$ nanocrystals with different shapes, such as: nanospheres, nanorods, and urchin-like microspheres were synthesized by a surfactant-free hydrothermal method. The as-obtained powders were characterized by X-ray diffraction patterns and transmission electron microscopy. XRD patterns indicate that these crystals have a wolframite-type monoclinic structure without deleterious phases. The TEM images revealed that the pH values and precursors played a key role in the morphology-controlled synthesis of $MnWO_4$ nanocrystals. This green method is an effective approach to the controlled growth of $MnWO_4$ nanocrystals with different shapes, which are of interest for both theoretical investigations and practical applications. Finally, a possible growth mechanism for the formation of the $MnWO_4$ microcrystals with different shapes was discussed in detail.

Keywords: Morphology-controlled synthesis; $MnWO_4$; Surfactant-free hydrothermal method

1. Introduction

Manganese tungstate ($MnWO_4$) is a very promising material due to its potential applications such as photocatalysts, optical fibers, photoluminescence, humidity sensors, and multiferroic materials [1–3]. Till now, $MnWO_4$ nanofibers, nanorods, nanowires, nanoflowers, nanoparticles, nanococoons have been prepared by various methods [4–10]. Recently, nanomaterials with controllable morphologies and sizes have drew much attention because of the strong correlation between these parameters and their properties and potential applications [11,12]. Specially, extensive work has been devoted to the investigation of efficient methods to prepare functional materials with complex three-dimensional nanostructures. Though urchin-like $MnWO_4$ microspheres have been successfully synthesized by the surfactant CTAB assisted hydrothermal method [13]. However, this method involved the disadvantage of complicated synthetic steps and was not environment friendly. Now, it is still a significant challenge for material researchers to synthesize urchin-like $MnWO_4$ microspheres by a simple and mild process.

In our previous work, our group has successfully synthesized $PbWO_4$ dendrites by a simple sonochemical method [14]. Therefore, in this paper, $MnWO_4$ nanorods, nanoparticles, and urchin-like microspheres were selectively prepared by a simple hydrothermal method without any templates or surfactants. Moreover, it is found that the obtained urchin-like $MnWO_4$ microspheres were composed of nanofibers, which is of fundamental importance in investigating the correlation between shape and basic physical properties. The present process is proved to be environment-friendly, and can be extended to the controllable synthesis of other tungstates.

2. Experimental details

In a typical experiment, sodium tungstate dihydrate [($Na_2WO_4 \cdot 2H_2O$), 99% purity, Aldrich], manganese chloride dihydrate [($MnCl_2 \cdot 2H_2O$), 99% purity, Aldrich], seignette salt [($C_4O_6H_4KNa$), 99% purity, Aldrich], citric acid trisodium salt

*Corresponding author. Tel.: +86 37 9659 28196.
E-mail address: wangyg968@163.com (Y. Wang).

0272-8842/$ - see front matter © 2013 Elsevier Ltd and Techna Group S.r.l. All rights reserved.
http://dx.doi.org/10.1016/j.ceramint.2013.09.117

dehydrate [($C_6H_5Na_3O_7 \cdot 2H_2O$), 99% purity, Aldrich], and sodium acetate trihydrate [(CH_3COONa), 99% purity, Aldrich] were used as the starting materials. First, equimolar amounts of seignette salt ($C_4O_6H_4KNa$), $MnCl_2$ and Na_2WO_4 were separately dissolved in distilled water to form aqueous solutions. Then, the first two solutions were mixed together with strongly magnetic stirring at room temperature, and a precipitate ($C_4H_4MnO_6$) was formed. The precipitate was filtered and washed with distilled water. Then, the resultant precipitate and Na_2WO_4 solution were transferred into a 50 mL stainless-steel autoclave for a hydrothermal treatment. The autoclave was sealed, heated to 200 °C and held for 3 h, and then cooled to room temperature naturally. The resultant precipitates were centrifuged, washed with distilled water, and dried naturally for characterization. The effect of pH values and precursors on the formation of $MnWO_4$ was investigated. The pH value of the mixed solution in the stainless-steel autoclave was adjusted to 5, 7, and 14, respectively. In addition, besides the precursor $C_4H_4MnO_6$, $(C_6H_5O_7)_2Mn_3$ and $(CH_3COO)_2Mn$ as precursors were prepared using citric acid trisodium salt dehydrate ($C_6H_5Na_3O_7.2H_2O$), sodium acetate trihydrate (CH_3COONa), and $MnCl_2$, respectively. And other reaction conditions were unchanged.

X-ray diffraction was performed on an X-ray diffractometer (D8 Focus, Germany) using CuKα radiation. Transmission electron microscope (TEM) images were taken with a JEOL, JEM-2100 by using an acceleration voltage of 200 kV.

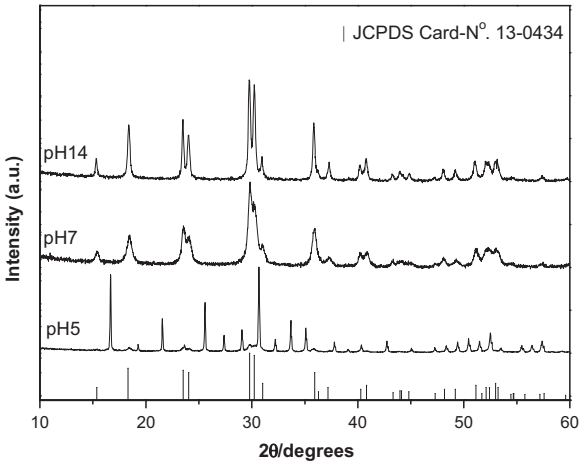

Fig. 1. XRD patterns of the as-prepared samples synthesized by the hydrothermal method using $(C_6H_5O_7)_2Mn_3$ and $Na_2WO_4 \cdot 2H_2O$ as precursors at different pH values (a) 5, (b) 7, and (c) 14, respectively.

3. Results and discussion

The effect of pH values on the formation of $MnWO_4$ nanocrystals was studied. Fig. 1 presents XRD patterns of the products prepared by the hydrothermal method using $(C_6H_5O_7)_2Mn_3$ and Na_2WO_4 as precursors at different pH values. The obtained product contained impurities in the case of pH5, as displayed in Fig. 1a. However, when the pH value was increased to 7 and 14 (Fig. 1b,c), it can be seen that all the diffraction peaks can be assigned to wolframite-type monoclinic structure in agreement with the respective Joint Committee on Powder Diffraction Standards (JCPDS) cards no.13-0434. Moreover, the diffraction peaks became stronger and sharper, which suggested that high pH value would be favorable for the crystallization and formation of pure $MnWO_4$ crystals.

Fig. 2 displays TEM images of the $MnWO_4$ nanocrystals synthesized by the hydrothermal method using $(C_6H_5O_7)_2Mn_3$ and $Na_2WO_4 \cdot 2H_2O$ as precursors at pH 7 and 14, respectively. As shown in Fig. 2(a), $MnWO_4$ nanocrystals with the mean particle size from 20 to 30 nm were obtained in the case of pH = 7. When the pH value was increased from 7 to 14, as depicted in Fig. 2(b), the particle sizes of the prepared $MnWO_4$ nanocrystals became obviously larger, which was consistent with the above XRD patterns.

The effect of precursors on the formation of $MnWO_4$ nanocrystals was also investigated. Fig. 3 exhibits the XRD patterns of the as-prepared samples synthesized by the hydrothermal method using $(CH_3COO)_2Mn$ and $Na_2WO_4 \cdot 2H_2O$ as precursors at different pH values. Impurities existed when the pH value was 5. As the pH value was increased to 7 and 14, all diffraction peaks can be assigned to a pure wolframite-type monoclinic structure with a space group (P2/c), point group symmetry (C_{2h}^4) and two clusters per unit cell ($Z = 2$) [15]. Based on the XRD patterns from Fig. 1 and Fig. 3, it can be concluded that low pH value was not favorable for the growing of nanocrystals to large $MnWO_4$ crystals.

Fig. 4 shows the TEM photographs of the $MnWO_4$ samples obtained by the hydrothermal method using $(CH_3COO)_2Mn$ and Na_2WO_4 as precursors at different pH values. It is

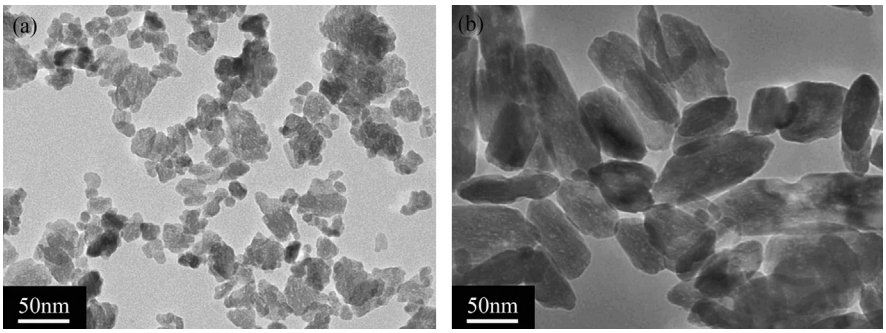

Fig. 2. TEM images of the as-prepared $MnWO_4$ samples synthesized by the hydrothermal method using $(C_6H_5O_7)_2Mn_3$ and $Na_2WO_4 \cdot 2H_2O$ as precursors at different pH values (a) 7 and (b) 14, respectively.

interesting to observe that the morphology of the $MnWO_4$ powders changes from sphericity with the mean particle size of 30 nm to rod shape with lengths of 300–400 nm and widths of 10–20 nm when the pH value was increased from 7 to 14. Obviously, increasing the pH value in the present hydrothermal process would promote the orientation growth of the $MnWO_4$ nanocrystals.

Fig. 5 displays the XRD patterns of the as-prepared samples synthesized by the hydrothermal method using $C_4H_4MnO_6$ and Na_2WO_4 as precursors at different pH values. It was clear that $MnWO_4$ phase with a monoclinic structure was prepared in the case of pH 5, but a small amount of impurity-phase was also detected. However, when the pH value was increased to 7 and 14, all the diffraction peaks can be indexed as pure $MnWO_4$ phase with a monoclinic structure, well consistent with the literature values (JCPDS no.13-0434). In addition, the broad and weak diffraction peaks indicated that the present precursors had an important influence on the crystallization and evolution of $MnWO_4$ nanocrystals.

Fig. 6 exhibits the typical TEM images of $MnWO_4$ samples prepared by the hydrothermal process using $C_4H_4MnO_6$ and Na_2WO_4 as precursors at different pH values. As shown in Fig. 6a, it is interesting to find that urchin-like $MnWO_4$ microspheres were formed in the case of pH 7. From the higher magnification TEM images in Fig. 6b, it can be seen that these microspheres were composed of abundant nanofibers with a length of 200–300 nm and a diameter of 4–5 nm, which corresponds with the broadening of the XRD peaks (Fig. 5b). When the pH value was increased from 7 to 14, similar urchin-like $MnWO_4$ microspheres with diameters of ca. 200–300 nm were obtained as shown in Fig. 6c. Fig. 6d clearly reveals the urchin-like structure of these $MnWO_4$ microspheres, from which it is observed that these microspheres consisted of abundant nanofibers. Furthermore, the aspect ratio of the nanofibers is larger than 40. The low-magnification TEM image (Fig. 6e) indicates that the obtained $MnWO_4$ products consist of a majority of such urchin-like nanostructures, revealing the high yield and favorable uniformity achieved through this approach.

To investigate the formation mechanism of the self-assembled urchin-like $MnWO_4$ microspheres, a series of time-dependent experiments were performed. As displayed in Fig. 7a and b, when the reaction time was 1 h and 2 h, respectively, only aggregates of nanorods with lengths of 20–30 nm and widths of 4–5 nm were obtained. However, as exhibited in Fig. 7c, it is interesting to find that urchin-like microspheres composed of nanofibers were formed when the reaction time was further prolonged to 3 h. Obviously, the formation of the urchin-like microspheres can be accounted for

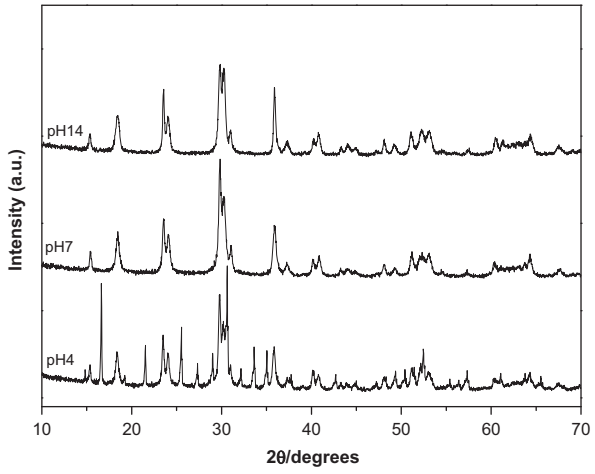

Fig. 3. XRD patterns of the as-prepared samples synthesized by the hydrothermal method using $(CH_3COO)_2Mn$ and $Na_2WO_4 \cdot 2H_2O$ as precursors at different pH values (a) 5, (b) 7, and (c) 14, respectively.

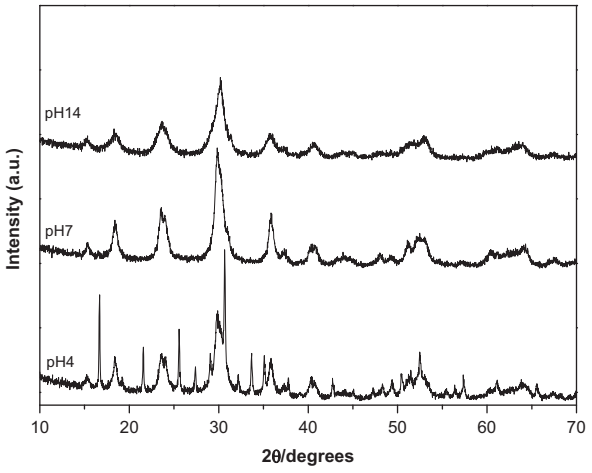

Fig. 5. Powder X-Ray diffraction patterns of the as-prepared samples synthesized by the hydrothermal method using $C_4H_4MnO_6$ and Na_2WO_4 as precursors at different pH values (a) 5, (b) 7, and (c) 14, respectively.

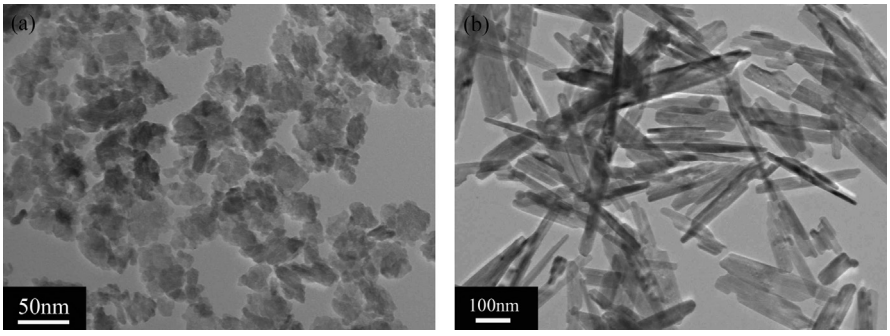

Fig. 4. TEM images of the as-prepared $MnWO_4$ samples synthesized by the hydrothermal method using $(CH_3COO)_2Mn$ and Na_2WO_4 as precursors at different pH values (a) 7 and (b) 14, respectively.

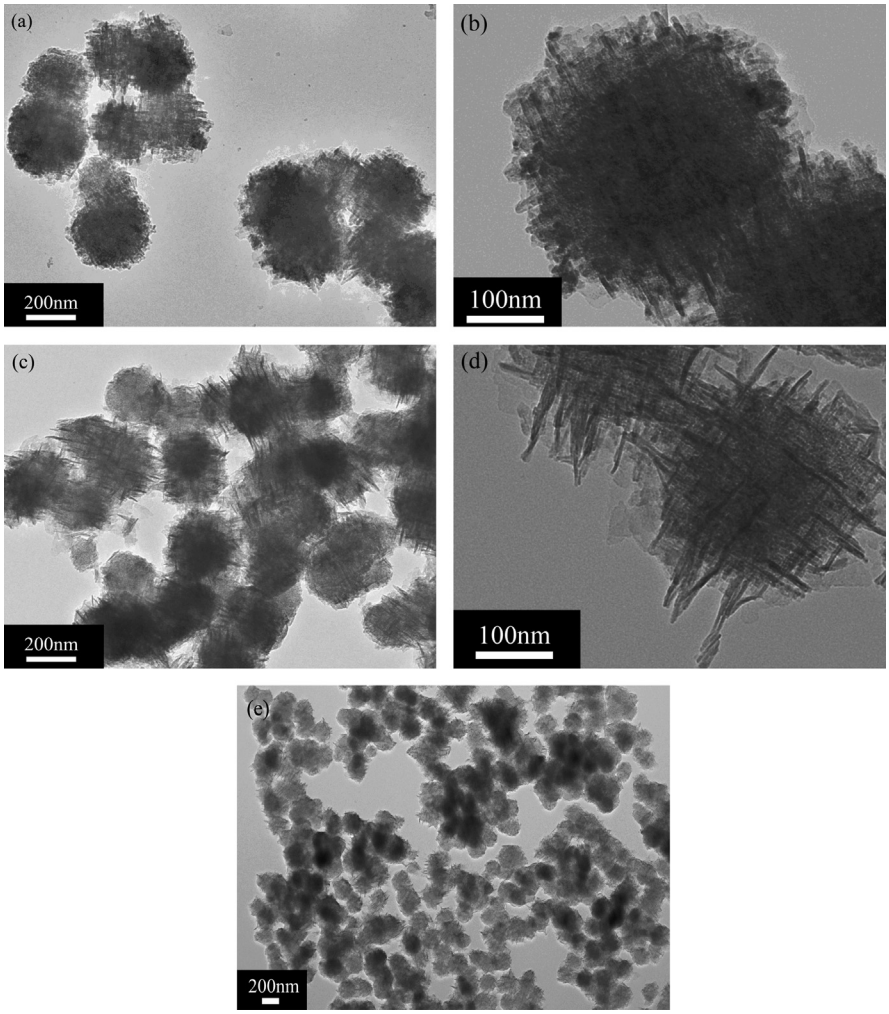

Fig. 6. TEM images of the as-prepared $MnWO_4$ samples synthesized by the hydrothermal method using $C_4H_4MnO_6$ and Na_2WO_4 as precursors at different pH values (a) 7, (b) a typical higher magnification TEM image of the as-prepared $MnWO_4$ nanocrystals, (c) 14, and (d) a typical higher magnification TEM image of the as-prepared $MnWO_4$ nanocrystals, respectively. (e) a typical low-magnification TEM image of the obtained $MnWO_4$ nanocrystals.

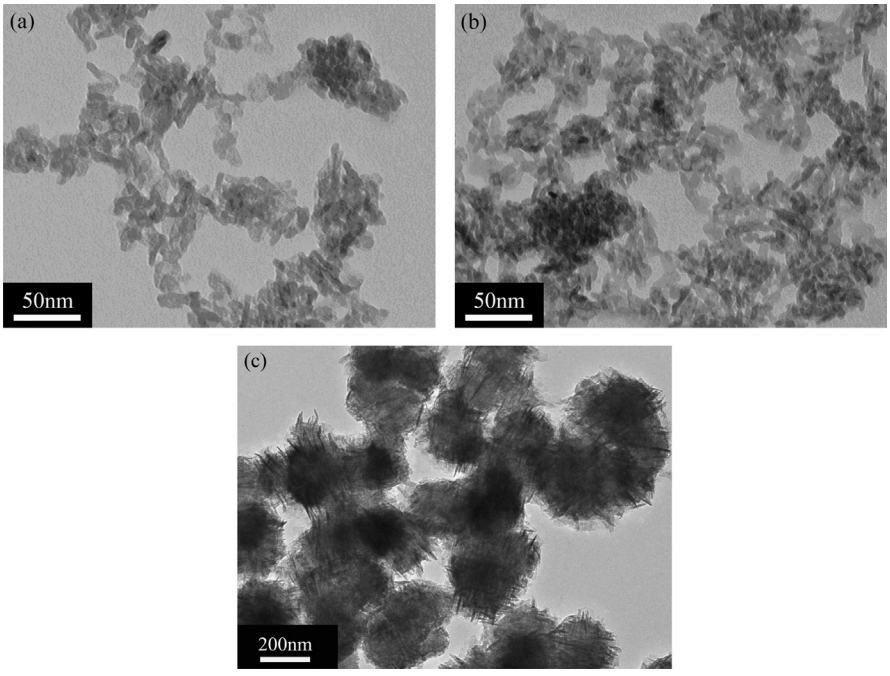

Fig. 7. TEM images of the as-prepared $MnWO_4$ samples synthesized by the hydrothermal method using $C_4H_4MnO_6$ and Na_2WO_4 as precursors at pH 14 for different reaction times: (a) 1 h, (b) 2 h, (c) 3 h, respectively.

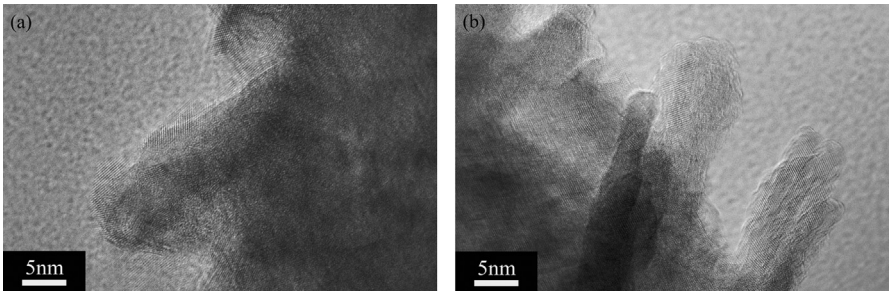

Fig. 8. HR-TEM images of the nanocrystals performed on the tip of as-prepared urchin-like $MnWO_4$ microspheres.

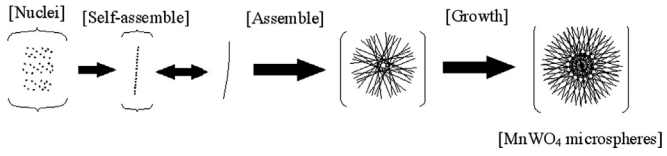

Fig. 9. Schematic illustration of the growth of urchin-like $MnWO_4$ microspheres.

by the self-assembly of nanofibers. Yu et al. have prepared urchin-like $MnWO_4$ microspheres assembled by nanorods with the assistance of CTAB [13]. However, in the present experiment, urchin-like $MnWO_4$ microspheres were successfully synthesized without any surfactants. The well known "oriented attachment" mechanism was proposed by Penn and Banfield et al. In this mechanism, the bigger particles are grown from small primary nanoparticles through an orientated attachment process. Although no surfactants or templates are added into the reaction system, we consider that $MnWO_4$ crystals may have a habit to be self-assembled through the orientated attachment process [16]. Fig. 8 shows the HR-TEM images of the nanocrystals on the tip of the obtained urchin-like $MnWO_4$ microspheres. It can be revealed that some nanocrystals are randomly aggregated (Fig. 8a) and others are oriented in similar crystallographic orientations (Fig. 8b), which suggests the presence of the aggregation process by an oriented attachment [17,18]. The formation process of the urchin-like $MnWO_4$ microspheres is illustrated schematically in Fig. 9. As the reaction mechanism is complicated, the exact reason for the shape-controlled synthesis of $MnWO_4$ crystals still needs to be further investigated.

4. Conclusions

We have developed a surfactant-free hydrothermal method for the shape-controlled synthesis of $MnWO_4$ nanocrystals, and $MnWO_4$ nanorods, nanoparticles, and urchin-like microspheres were successfully synthesized, respectively. It is found that the morphologies of the obtained $MnWO_4$ nanocrystals were strongly dependent on the pH values and precursors. The TEM and HR-TEM images indicated that urchin-like $MnWO_4$ microspheres were formed via self-assembly of nanofibers. This green method is an effective approach to the controlled growth of $MnWO_4$ nanocrystals with interesting morphologies, which are of interest for both theoretical investigations and practical applications.

Acknowledgments

This work is supported by the Natural Foundation of the Education Department of Henan Province (2011B430019) and the Doctor Foundation of Luoyang Institute of Science and Technology (2009BZ05).

References

[1] S. Thongtem, S. Wannapop, A. Phuruangrat, T. Thongtem, Cyclic microwave-assisted spray synthesis of nanostructured $MnWO_4$, Materials Letters 63 (2009) 833–836.
[2] H.Y. He, J.F. Huang, L.Y. Cao, J.P. Wu, Photodegradation of methyl orange aqueous on $MnWO_4$ powder under different light resources and initial pH, Desalination 252 (2010) 66–70.
[3] L.H. Hoang, N.T.M. Hien, W.S. Choi, Y.S. Lee, K. Taniguchi, T. Arima, S. Yoon, X.B. Chen, I.S. Yang, Temperature-dependent Raman scattering study of multiferroic $MnWO_4$, Journal of Raman Spectroscopy 41 (2010) 1005–1010.
[4] S. Saranya, S.T. Senthilkumar, K. Vijaya Sankar, R. Kalai Selvan, Synthesis of $MnWO_4$ nanorods and its electrical and electrochemical properties, Journal of Electroceramics 28 (2012) 220–225.
[5] S. Lei, K. Tang, Z. Fang, Y. Huang, H. Zheng, Synthesis of $MnWO_4$ nanofibres by a surfactant-assisted complexation precipitation approach and control of morphology, Journal of Nanotechnology 16 (2005) 2407–2411.
[6] T.D. Nguyen, D. Mrabet, T.T. Duong Vu, C.T. Dinh, T.O. Do, Biomolecule-assisted route for shape-controlled synthesis of single-crystalline MnWO4 nanoparticles and spontaneous assembly of polypeptide-stabilized mesocrystal microspheres, CrystEngComm 13 (2011) 1450–1460.
[7] M.A.P. Almeida, L.S. Cavalcante, J.A. Varela, M. Siu Li, E. Longo, Effect of different surfactants on the shape, growth and photoluminescence behavior of $MnWO_4$ crystals synthesized by the microwave-hydrothermal method, Advanced Powder Technology 23 (2012) 124–128.
[8] Y. Xing, S. Song, J. Feng, Y. Lei, M. Li, H. Zhang, Microemulsion-mediated solvothermal synthesis and photoluminescent property of 3D flowerlike $MnWO_4$ micro/nanocomposite structure, Solid State Sciences 10 (2008) 1299–1304.
[9] H.J. Zhou, Y.E. Yiu, M.C. Aronson, S.S. Wong, Ambient template synthesis of multiferroic $MnWO_4$ nanowires and nanowire arrays, Journal of Solid State Chemistry 181 (2008) 1539–1545.
[10] S. Thongtem, S. Wannapop, T. Thongtem, Characterization of $MnWO_4$ with flower-like clusters produced using spray pyrolysis, Transactions of Nonferrous Metals Society of China 19 (2009) s100–s104.
[11] H.G. Yang, C.H. Sun, S.Z. Qiao, J. Zou, G. Liu, S.C. Smith, et al., Anatase TiO_2 single crystals with a large percentage of reactive facets, Nature 453 (2008) 638–641.
[12] C.B. Burda, X.B. Chen, R. Narayanan, M.A.E. Sayed, The chemistry and properties of nanocrystals of different shapes, Chemical Reviews 105 (2005) 1025–1102.

[13] Y.X. Zhou, Q. Zhang, J.Y. Gong, S.H. Yu, Surfactant-assisted hydrothermal synthesis and magnetic properties of urchin-like $MnWO_4$ microspheres, Journal of Physical Chemistry C 112 (2008) 13383–13389.

[14] Y.G. Wang, L.L. Yang, Y.J. Wang, X.F. Wang, L.J. Wang, Facile electrochemical synthesis of $PbWO_4$ dendrites, Ceramics International 39 (2013) 8481–8486.

[15] M.A.P. Almeida, L.S. Cavalcante, M.S. Li, J.A. Varela, E. Longo, Structural refinement and photoluminescence properties of $MnWO_4$ nanorods obtained by microwave-hydrothermal synthesis, Journal of Inorganic and Organometallic Polymers 22 (2012) 264–271.

[16] L.S. Cavalcante, V.M. Longo, J.C. Sczancoski, M.A.P. Almeida, A.A. Batista, J.A. Varela, et al., Electronic structure, growth mechanism and photoluminescence of $CaWO_4$ crystals, CrystEngComm 14 (2012) 853–868.

[17] M.A.P. Almeida, L.S. Cavalcante, C. Morilla-Santos, P.N. Lisboa Filho, A. Beltrán, J. Andrés, et al., Electronic structure and magnetic properties of $FeWO_4$ nanocrystals synthesized by the microwave-hydrothermal method, Materials Characterization 73 (2012) 124–129.

[18] V.S. Marques, L.S. Cavalcante, J.C. Sczancoski, A.F.P. Alcantara, M.O. Orlandi, E. Moraes, et al., Effect of different solvent ratios (water/ethylene glycol) on the growth process of $CaMoO_4$ crystals and their optical properties, Crystal Growth and Design 10 (11) (2010) 4752–4768.